Energy 266 (2023) 126352

Contents lists available at ScienceDirect

Energy

journal homepage: www.elsevier.com/locate/energy

Comparative thermodynamic analysis of an improved ORC process with integrated injection of process fluid

Jürgen Krail [a,*], Georg Beckmann [b], Florian Schittl [a], Gerhard Piringer [a]

[a] Josef Ressel Centre for Linked System Assessment to Support Sustainable Energy Supplies (LiSA)Department of Energy & Environment, University of Applied Sciences Burgenland, Pinkafeld, Austria

[b] Technical Office for Mechanical and Energy Engineering Beckmann, Vienna, Austria

ARTICLE INFO

Keywords:
Waste heat recovery
Organic Rankine Cycle (ORC)
Process simulation
Improved process design
Process efficiency

ABSTRACT

In contrast to water-steam Rankine cycles, the ORC process uses organic working fluids. For working fluids of the dry class, a recuperator heat exchanger is frequently installed to increase the cycle efficiency. This paper analyses an improved ORC process with these features: A liquid working fluid stream is injected into the vapour flow between the high-pressure and the medium-pressure stage of the turbine. Furthermore, the recuperator is replaced by a spray condenser. The main objective is to increase efficiency with moderate changes in the process layout. A thermodynamic comparison of the improved process with a state-of-the-art ORC process is carried out by simulations and optimisations. A significant efficiency gain for the improved ORC process is obtained by a combination of the aforementioned features, mainly because of an increase of the mass flow in the economiser of the vapour generator (better heat utilization) and a corresponding mass flow in the medium stage of the turbine (additional power production). As a use case, waste heat utilization from a clinker cooler at a temperature level of 275 °C was simulated. The improved process would lead to a significant increase in the overall net efficiency by up to 14%, compared to a state-of-the-art ORC process.

1. Introduction

1.1. ORC processes

Electricity generation from low-temperature heat, such as waste heat, represents a significant contribution to fossil fuel substitution and a reduction in the CO_2 intensity of energy supply. Around 50% of global energy consumption is expected to end up as waste heat by 2030 [1]. Economically viable waste heat utilization will thus play a substantial position in the energy transition. A number of studies estimate a high potential of useable waste heat [2–4].

One of the most promising options for the conversion of waste heat to electricity is the Organic Rankine Cycle (ORC) process. In Europe, the waste heat suitable for conversion by ORC plants is estimated to be around 20 TWh, which corresponds to CO_2 emissions savings of around 7.6 million tonnes [5]. Besides industrial waste heat utilization, ORC processes are also used for electricity generation in the fields of geothermal energy, biomass, or solar thermal energy. The annual installed capacity of ORC plants has steadily increased over the last 15 years. At the end of 2016, 1754 plants with a total installed capacity of around 2.70 GW were installed worldwide [6]. By 2020, the cumulated global installed capacity had increased to 4.07 GW, with geothermal applications achieving the highest cumulative capacity growth (+970 MW, +45%) from 2016 to 2020, whereas waste heat recovery applications achieved the highest growth in terms of installed units (+628 plants, +207%) [7].

Suggestions for improving this technology are expected to require more complex and sophisticated power plant cycles [8]. However, to expand the useable potential of low-temperature heat, the market also requires, among other things, an entry-level technology, cost efficiency, acceptance by operators and an ability to utilize low-exergy sources [9].

Abbreviations: A, auxiliary units (electric motors for fansand pumps); B, boiler; C, cycle; CO, condenser; CC, condensate cooler; CP, condensate pump; EL, electric; EV, evaporator; FA, fan; FP, feed pump; G, generator; I, mean values state parameters inlet; IN, inlet stream; IS, isentropic; HP, high pressure stage; HS, heat source; M, mechanic; NET, net value; LP, low pressure (exhaust vapour); MI, mixing chamber; MIN, minimum; MO, motor; MP, medium pressure stage; O, mean values state parameters outlet; OUT, outlet stream; PH, preheater; PU, pump; R, recuperator; REF, reference conditions; REL, relative; TO, thermo oil; TOB, thermo oil boiler; TOP, thermo oil pump; TU, turbine; VG, vapour generator; WF, working fluid; WHS, waste heat source; WHR, waste heat recovery.

* Corresponding author.
E-mail address: juergen.krail@fh-burgenland.at (J. Krail).

https://doi.org/10.1016/j.energy.2022.126352
Received 1 March 2022; Received in revised form 29 October 2022; Accepted 4 December 2022
Available online 6 December 2022

Nomenclature

η	efficiency (%)
g	acceleration of gravity (m/s^2)
h	enthalpy (kJ/kg)
$\dot{m}$	mass flow (kg/s)
P	electrical power (kW)
p	pressure (bar)
$\dot{Q}$	thermal power (kW)
v	velocity (m/s)
W	mechanical power (kW)
s	entropy (kJ/kgK)
T	temperature (°C)
x	vapour quality (−)
z	geodetic altitude (m)

The ORC technology can be adapted to different heat sources by matching an appropriate working fluid to the source's temperature. This results in a wide range of applications, with a minimum source temperature of approximately 80 °C. Output power ranges from small plants with an electrical output of a few kW to power plants in the double-digit MW range [10–13].

The subcritical ORC process is well established in electricity generation from waste heat and also in geothermal plants [14]. More recent ORC technologies propose the following efficiency-enhancing developments:

- Selection of the process fluid:
  - selection procedures [15,16].
  - zeotropic fluid mixtures [17,18].
- Process design:
  - dual-pressure processes [19,20].
  - dual-loop processes [21–23].
  - novel ORC architectures for waste heat recovery [8].
  - trans- and supercritical process design [24–26].
- Optimisation of the process components [27,28] and the use of novel process components [8,29].
- Advanced control strategies [30–33].

Comparative studies regarding zeotropic fluid mixtures show partly lower, partly moderately higher (up to 1.6%) net efficiencies [34–36]. However, this efficiency improvement is often associated with a need for a larger heat transfer area [37] and thus increased costs [38]. Adjusting the concentration during operation, for example to the outside temperature, can noticeably improve the average annual efficiency [39,40]. Zeotropic mixtures also complicate requirements for the vapour generator and condenser heat exchanger.

In two-stage processes, which can also lead to an increase in efficiency, vapour generation takes place at two different temperature levels [41–43]. The supercritical process shows efficiency advantages for heat sources with temperatures above 300 °C [44]. Suitable working fluids (e.g. R1233zd) improve the cycle efficiency [45].

Literature estimates of the (relative) efficiency gains achievable by the measures mentioned above do not exceed 15%, compared to the conventional subcritical ORC process. However, each of these measures requires additional design development or additional modifications to the plant design as a whole.

1.2. *Improved ORC process design*

The improved cycle aims at a relative increase of the overall efficiency beyond 10%, using common components. Unconventional ways of removing condensation heat and of extracting useful heat are central features of the proposed thermodynamic cycle. Nevertheless, well-known process steps (e.g., desuperheating by means of liquid injection) are used. The basic idea of the invention can be applied to a wide variety of designs, from highly efficient to cost-optimised, multi-purpose systems, with a wide range of power generated.

The improved ORC process design (Fig. 1, right) is characterized by preheated working fluid being injected into the vapour flow between the high-pressure and medium-pressure stage of the turbine at the MI MP (mixing chamber, medium pressure) stage. In a further step, mixing takes place also after the medium pressure MI LP (mixing chamber, low pressure (exhaust vapour)) stage of the turbine, before the condenser. This renders unnecessary the recuperator heat exchanger that is usually part of a state-of-the art ORC process (component R in Fig. 1, left). Furthermore, the mass flow of the working fluid increases in the preheater and in the medium pressure stage of the turbine, which leads to a higher energy output and an increase of the overall cycle efficiency.

The additional requirements, relative to a common ORC, are:

a. The use of a turbine with two casings (similar to a steam reheat turbine)
b. The introduction of desuperheating at the intermediate pressure level to increase efficiency (spray desuperheating is a widely used component in steam power plants to control temperatures)
c. The additional introduction of desuperheating at the low-pressure level, before condensation, to enhance heat transfer at the condenser
d. The provision of a preheater with a somewhat larger heat transfer surface

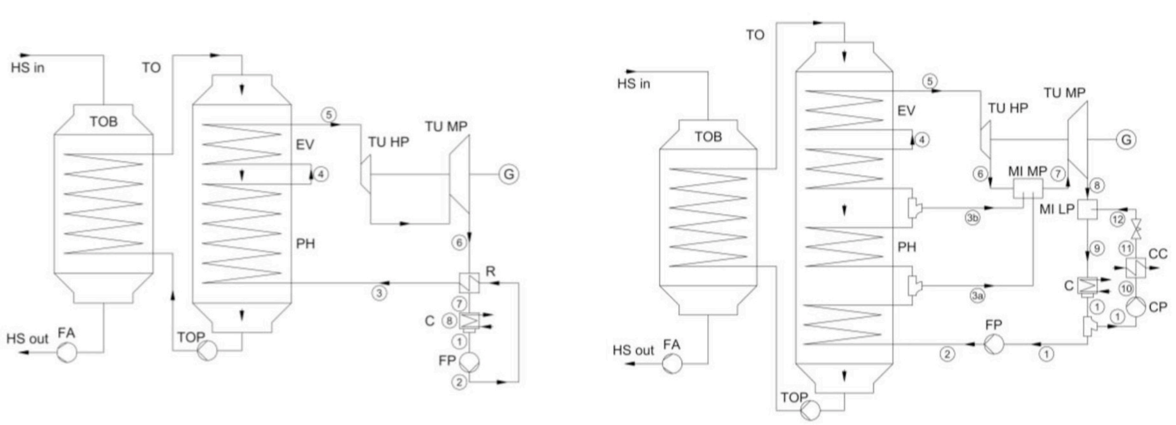

Fig. 1. Flow diagram of a state-of-the-art ORC process (left), and of the improved ORC process (right), both applied to waste heat recovery from exhaust air from a clinker cooler.

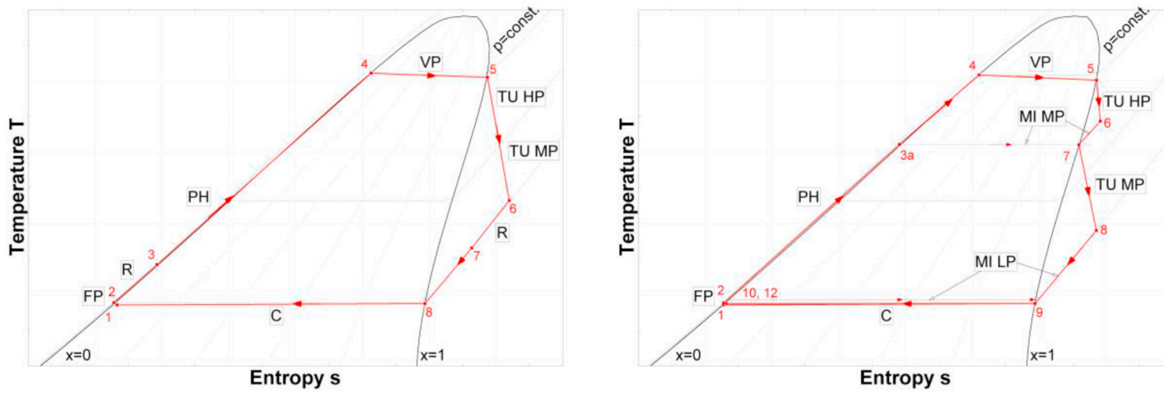

Fig. 2. T-s Diagram of the state-of-the-art ORC process (left) and the improved ORC process (right).

e. The optional replacement of the shell and tube condenser by a spray condenser (an occasionally used technology in steam power plants with a dry cooling tower system), combining desuperheating and condensation in one component.

Point a. appears to be the largest requirement; on the other hand, a turbine with two casings paves the way to combined heat and power generation in waste heat recovery. Also on the positive side, the use of condenser-side options may lead to a process simplification.

A patent application has been filed for this improved process design, and a national (Austrian) patent [46] has already been granted; the international patent application [47] is pending.

To illustrate the thermodynamic advantages of the improved ORC process design, Fig. 2 compares the T-s diagram of the two ORC processes for the working fluid n-pentane.

Dry class working fluids are characterised by a superheated exhaust vapour state after expansion (Fig. 2 (left) – state point 6; Fig. 2 (right) – state point 6, 8). This has the advantage that the vapour does not have to be superheated before entering the turbine, which is particularly relevant for low-temperature processes. However, this overheating of the exhaust vapour at the turbine outlet has thermodynamic disadvantages, which are partly compensated by a recuperator heat exchanger in state-of-the-art processes (Fig. 1 (left) – component R; Fig. 2 (left) – state points 6–7 → 2–3).

In the improved ORC process the superheating of the turbine exhaust vapour is reduced by adding working fluid after the high-pressure stage of the turbine (Fig. 1 (right) – component MI MP; Fig. 2 (right) – state points 6 + 3a → 7). This is carried out until the state of the vapour entering the medium pressure stage of the turbine is on the saturated vapour line (Fig. 2 (right) – state point 7). This increases the mass flow through the medium-pressure stage of the turbine (TU MP), resulting in a higher turbine power output. Furthermore, working fluid is again added after the turbine's medium pressure stage in the form of a spray condenser (Fig. 1 (right) – component MI LP; Fig. 2 (right) – state points 8 + 12 → 9), which avoids the need for a recuperator in the improved ORC process. The absence of the recuperator's pressure loss allows expansion to a lower exhaust vapour pressure level (Fig. 2 (right) – state point 8), compared to the state-of-the-art ORC process (Fig. 2 (left) – state point 6). This leads to a higher enthalpy gradient at the turbine stages, which increases the turbine power output. For simplicity, the improved ORC process is shown in Fig. 2 with only one mixing step (3a) and without a condensate cooler (CC).

2. Materials and methods

2.1. Energy balance and process efficiency

The thermodynamic simulation of both investigated ORC processes was based on mass and energy balances for steady state flow processes, according to Eqs. (1) and (2), according to Ref. [48]. The index "IN" stands for the mass and energy flows entering the system and the index "OUT" for the energy and mass flows leaving the system, the index "I" stands for the cross-sectional mean values of the state values of the fluid in the inlet cross section and the index "O" stands for the cross-sectional mean values of the state values of the fluid in the outlet cross section. In the calculations carried out, the velocity momentum and the geodetic altitude were neglected, so that the equation can be simplified according to Eq. (3). In the following calculations, heat losses are neglected for all components (units and pipes). The pressure drop was calculated for heat exchangers, but assumed to be zero for pipes.

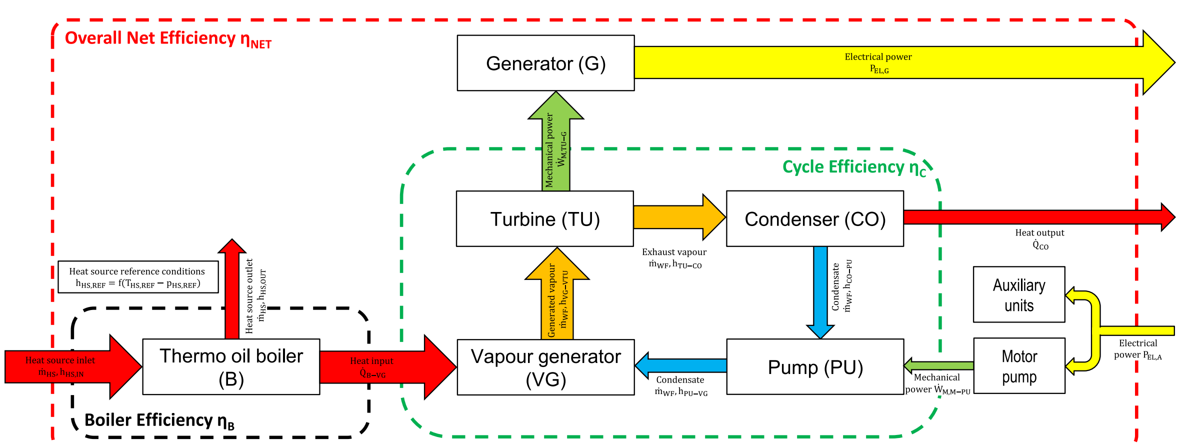

Fig. 3. Energy balance and efficiency coefficients.

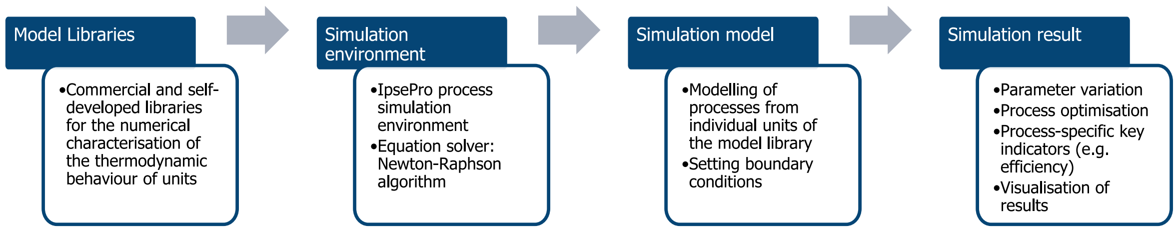

Fig. 4. Structure of the process simulation in IPSEpro.

$$\sum_{IN}\dot{m}_I = \sum_{OUT}\dot{m}_O \tag{1}$$

$$\dot{Q} + P = \sum_{OUT}\dot{m}_O\left(h + \frac{w^2}{2} + g\,z\right)_O - \sum_{IN}\dot{m}_I\left(h + \frac{w^2}{2} + g\,z\right)_I \tag{2}$$

$$\dot{Q} + P = \sum_{OUT}\dot{m}_O h_O - \sum_{IN}\dot{m}_I h_I \tag{3}$$

The process evaluation was carried out on the basis of efficiency coefficients (Fig. 3). In addition to the overall net efficiency η_{NET}, the individual efficiency coefficients of the vapour generator η_B and the thermodynamic cycle η_C were also calculated.

The efficiency of the thermo oil boiler η_B was calculated according to Eq. (4). Since waste heat is assumed as the heat source for the investigated processes, the thermal power input into the vapour generator $\dot{Q}_{HS-REF}$ was assigned reference conditions ($T_{HS,REF} = 25\ ^\circ C$, $p_{HS,REF} = 1.013$ bar) that are commonly used in power plant engineering. The output is defined as the thermal power transferred to the cycle $\dot{Q}_{B-VG}$, with heat losses neglected for the vapour generator and for all heat exchangers and pipes.

$$\eta_B = \frac{\dot{Q}_{B-VG}}{\dot{Q}_{HS-REF}} = \frac{\dot{m}_{WF}\left(h_{VG-TU} - h_{PU-VG}\right)}{\dot{m}_{HS}\left(h_{HS,IN} - h_{HS,REF}\right)} \tag{4}$$

The cycle efficiency η_C describes the internal energy conversion of the process without taking into account the utilization of the available heat source. For the calculation of cycle efficiency, the output of the expansion machine $\dot{W}_{TU-G}$ minus the power for the pump operation $\dot{W}_{M-PU}$ was considered as the useful power Eq. (5). The input power is the thermal power of the vapour generator $\dot{Q}_{B-VG}$.

$$\eta_C = \frac{\dot{W}_{TU-G} - \dot{W}_{M-PU}}{\dot{Q}_{B-VG}} = \frac{\dot{m}_{WF}\left(h_{VG-TU} - h_{TU-C}\right) - \dot{m}_{WF}\left(h_{PU-VG} - h_{CO-PU}\right)}{\dot{m}_{WF}\left(h_{VG-TU} - h_{PU-VG}\right)} \tag{5}$$

Although the use case investigated here is a process where the heat source is available as waste heat, it is appropriate for economic reasons to consider the overall net efficiency η_{NET} as the most relevant criterion for the process comparison with a conventional state-of-the-art ORC process. It relates the net electrical output of the process $P_{EL,G} - \sum P_{EL,A}$ to the amount of waste heat based on the reference conditions $\dot{Q}_{HS-REF}$ and represents the "yield" of electrical power from an existing/available waste heat source (Eq. (6)). For the net electrical output of the process, all outputs for operating auxiliary units $\sum P_{EL,A}$ were subtracted from the electrical output of the generator $P_{EL,G}$. The auxiliary units were the pump for the working fluid, the thermal oil pump, as well as the electrical power for the fan of the air condenser and the electrical power for the waste heat fan for covering the pressure loss of the thermo oil boiler.

$$\eta_{NET} = \frac{P_{EL,G} - \sum P_{EL,A}}{\dot{Q}_{HS-REF}} = \frac{P_{EL,G} - \sum P_{EL,A}}{\dot{m}_{HS}\left(h_{HS,IN} - h_{HS,REF}\right)} \tag{6}$$

2.2. Process simulation

The simulation of the processes was carried out with the commercial software IPSEpro [49]. Fig. 4 describes the steps involved. In the model library, the individual units that are used to design the process are described with thermodynamic mass and energy balance equations. The IPSEpro library for low-temperature processes "LTP-Lib -

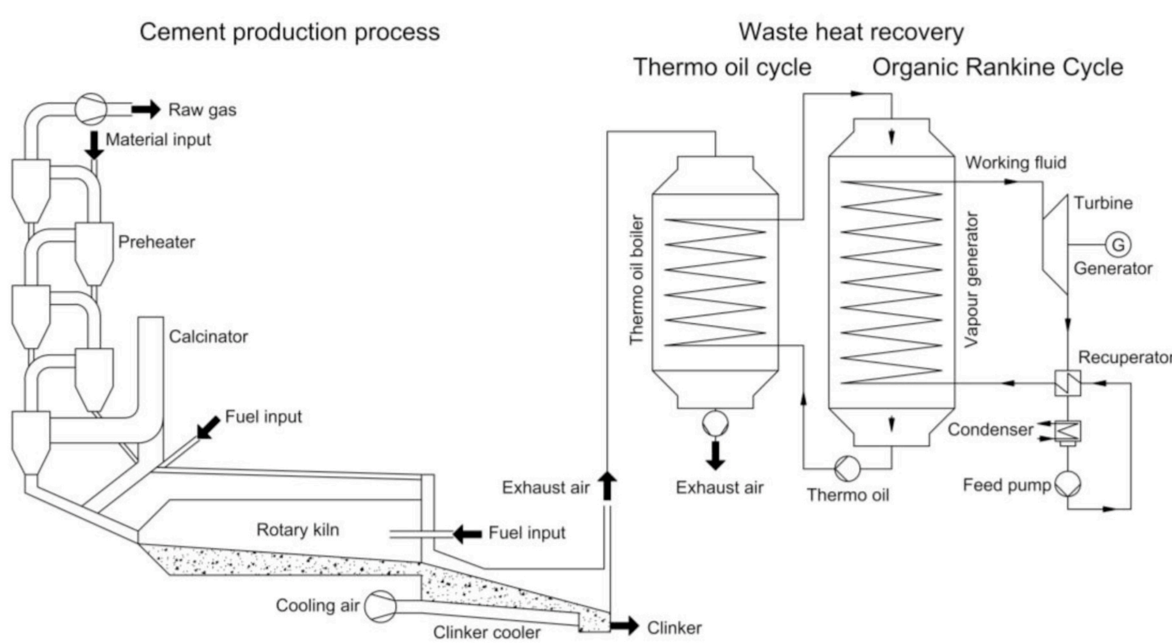

Fig. 5. Design of an ORC waste heat recovery process in a cement production plant by using exhaust air from the clinker cooler (based in part on [58]).

Table 1
Boundary conditions.

	State-of-the-art ORC process[a]	Improved ORC process	Unit
Waste heat input (hot air from clinker cooler)			
Waste heat input – temperature $T_{HS,IN}$	275	275	°C
Waste heat input – mass flow $\dot{m}_{HS}$	55	55	kg/s
Waste heat input – thermal power $\dot{Q}_{HS-REF}$[b]	14,000	14,000	kW
ORC process			
Working fluid	n-Pentane	n-Pentane	
Thermo oil boiler – min. temp. difference $\Delta T_{TOB,MIN}$	37.9	37.9	K
Vapour generator – min. temp. difference $\Delta T_{VG,MIN}$	14.0	14.0	K
Recuperator – min. temp. difference $\Delta T_{R,MIN}$	28.9	–	K
Generator – electric efficiency $\eta_{EL,G}$	98.0	98.0	%
Generator – mechanic efficiency $\eta_{M,G}$	97.0	97.0	%
Motor – electric efficiency $\eta_{EL,MO}$	95.0	95.0	%
Motor – mechanic efficiency $\eta_{M,MO}$	97.0	97.0	%
Pump – isentropic efficiency $\eta_{IS,PU}$	78.5	78.5	%
Pump – mechanic efficiency $\eta_{M,PU}$	97.0	97.0	%
Turbine – isentropic efficiency $\eta_{IS,TU}$[c]	74.5	74.5	%
Turbine – mechanic efficiency $\eta_{M,TU}$	98.0	98.0	%
Turbine – exhaust vapour pressure $p_{TU,OUT}$[d]	1.03	0.98	bar
Condenser (cooling medium ambient air)			
Condenser inlet – temperature $T_{CO,IN}$	11	11	°C
Condenser outlet – temperature $T_{CO,OUT}$	33	33	°C

[a] State-of-the-art ORC process, boundary conditions based on Heidelberger Cement AG [56] and Umweltbundesamt [57].
[b] Based on reference conditions $T_{HS,REF} = 25$ °C and $p_{HS,REF} = 1.013$ bar.
[c] The isentropic efficiency applies to both stages of the turbine.
[d] The lack of a recuperator-caused pressure loss in the improved process causes a lower exhaust vapour pressure at the turbine outlet.

Low-Temperature Processes" [50] was used as model library. Furthermore, the thermodynamic fluid properties are also calculated in the model library. The database used for calculation is the "RefProp" database [51].

IPSEpro "PSE - Process Simulation Environment" [52] offers a visual programming interface for the modelling, simulation and optimisation of thermodynamic cycles. The IPSEpro equation solver, which is part of the simulation environment, is based on a Newton-Raphson algorithm [53]. The optimisation module "PSOptimize" [54] allows process multivariate optimisation. Free equations can be used to define additional variables, e.g. for the calculation of efficiency coefficients. By means of the additional module "PSXLink" [55], parameter variations can be carried out in Excel.

In the simulation model, the processes to be analysed are designed based on units available in the model library, and then appropriate boundary conditions are added.

The simulation result delivers the results of the parameter variation and the process optimisation based on process-specific indicators, such as efficiency factors. Furthermore, simulation results can be displayed as diagrams (e.g. T-s diagram).

2.3. Comparison of the improved ORC process with the state-of-the-art ORC process

To compare the two ORC processes under investigation, a waste heat recovery process in a cement production plant was taken as a use case (Fig. 5). In this use case, the exhaust air from the clinker cooler is utilised for electricity production. The use case is based on a real plant, which is documented in reports by Heidelberger Cement AG [56] and defined by the German Environment Agency [57] as Best Available Technique in the Cement, Lime and Magnesium Oxide Industry.

After the exhaust air leaves the clinker cooler at a temperature of 275 °C, it is led to the thermo oil boiler, where the heat of the exhaust air is transferred to the thermo oil cycle. The thermo oil cycle is interposed in the ORC process for safety reasons. The exhaust air exits the thermo oil boiler at a lower temperature level and is transported by means of an induced draught fan to downstream filters (not shown in the illustration). The thermo oil cycle transports the heat to the vapour generator, where it preheats and evaporates the working fluid to the saturation line in a counter current flow arrangement. Afterwards, in a downstream ORC process, the thermal energy is converted into mechanical energy and subsequently into electrical energy.

The suitability and advantages of the improved ORC technology depend on boundary conditions and parameters that are specific for each project, process, and plant. First, there is the selection of the working fluid. As already mentioned, the thermodynamic advantages are predicated on organic working fluids of the dry class, but even within this class, the entropy reductions at the saturated vapour line during expansion can vary. Another determining factor is the waste heat source itself, with its yield and temperature. Current research is not known to allow generally valid and quantifiable statements about the thermodynamic advantages with a wide range of parameters and parameter combinations. Therefore, the following comparison is based on an operational and comprehensively documented, state-of-the-art ORC plant for electricity generation from hot air from the clinker cooler of a cement factory [56,57]. The improved ORC process is designed for this same application.

In order to ensure an equal comparison between the two ORC process designs, the same boundary conditions were set (Table 1). The simulations presented here refer to an input waste heat stream at 275 °C and a thermal power input of 14 MW, based on reference conditions. n-pentane is used as the working fluid in the state-of-the-art process, and so it was also chosen for the improved design. The isentropic efficiency of the turbine was calculated on the basis of design data from Heidelberger Cement AG [56] and subsequently assumed to be 74.5% for both comparative processes in the respective turbine stages. On the heat sink side, an ambient temperature of 11 °C was assumed in each case. The thermodynamic comparability of the heat exchangers was ensured by assuming the same minimum temperature difference between the hot and cold fluid of the heat exchanger. Since the recuperator is no longer required in the improved process, the turbine can expand to a lower condensation pressure by omitting the pressure drop of the recuperator.

Parameter studies were carried out for the two processes, whereby both processes were investigated with a focus on maximising the overall net efficiency η_{NET}, using the IpsePro optimisation algorithm PSOptimize. While the process-external boundary conditions were kept constant (see Table 1), the vapour pressure entering the high-pressure stage of the turbine (Figs. 1 and 2 – state point 5) was varied. In the case of the improved process, for each pressure variation of the vapour pressure entering the high-pressure stage of the turbine, the pressure level of the intermediate pressure (Fig. 1 (right) and Fig. 2 (right) – state point 7) was also optimised with a focus on maximising the net overall efficiency η_{NET}. In both cases, the pressure variation of the vapour was carried out in the subcritical pressure range of the working fluid n-pentane. Based on these simulations, an optimum vapour pressure was calculated for each individual process in order to reach a maximum overall net-efficiency.

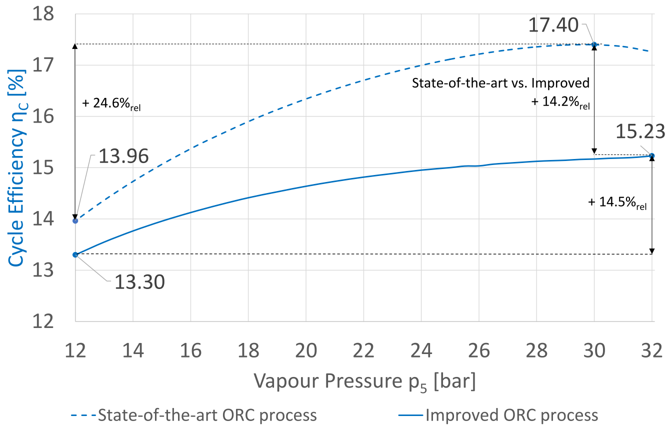

Fig. 6. Cycle efficiency of the state-of-the-art ORC process (dashed line) and the improved ORC process (solid line) as a function of the vapour pressure.

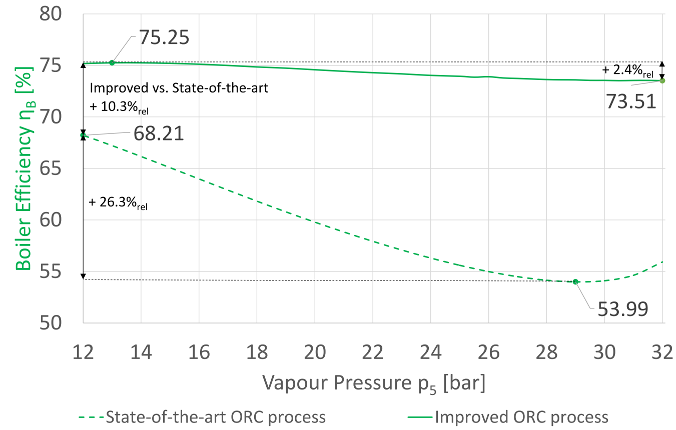

Fig. 7. Boiler efficiency of the state-of-the-art ORC process (dashed line) and the improved ORC process (solid line) as a function of the vapour pressure.

3. Results

To better explain the simulation results, the influence of the optimal vapour pressure on the cycle efficiency η_C and the boiler efficiency η_B is first considered separately. The influence on the net overall efficiency η_{NET} is then summarised in a separate chapter.

3.1. Cycle efficiency

An increase in live steam pressure and temperature is cited in the thermodynamics literature for water-steam Rankine cycles as a possible measure for increasing the cycle efficiency [48,59,60]. The increase of the live steam temperature is technically limited due to the temperature level of the heat source and the temperature durability of the boiler materials.

As an intermediate result of the comparative simulations, Fig. 6 shows the cycle efficiencies according to Eq. (4) of the state-of-the-art ORC process and of the improved ORC process, both as a function of the vapour pressure. As in conventional water-steam Rankine cycles, the cycle efficiency of the state-of-the-art ORC process increases with rising vapour pressure. At the same time, the degree of superheating of the exhaust vapour at the turbine outlet increases with increasing vapour pressure, which has a negative effect on the cycle efficiency. At pressures above appr. 30 bar, this negative influence of the increased superheating in the turbine exhaust vapour outweighs the increase in efficiency due to the increased live vapour pressure. As a result, the cycle efficiency of the process decreases in this pressure range. The maximum cycle efficiency of the state-of-the-art process is 17.4%, which is reached at a vapour pressure of 30 bar. The relative increase in cycle efficiency in the pressure range investigated is 24.6%$_{rel}$ for the state-of-the-art ORC process.

The improved ORC process shows a similar trend. In the comparison between the two cycles investigated, however, the cycle efficiency increases only moderately with increasing vapour pressure and reaches its maximum at the maximum vapour pressure of 32 bar, close to the critical pressure, at 15.23%. The percentage increase in cycle efficiency in the pressure range investigated is 14.5%$_{rel}$ for the improved ORC process. If cycle efficiency is used as the only criterion for process evaluation, it becomes evident that at optimum vapour pressure the state-of-the-art process shows a 14.2%$_{rel}$ higher cycle efficiency than the improved ORC process.

However, further considerations of the boiler efficiency and the resulting overall net efficiency show that cycle efficiency is not sufficiently meaningful as a decision criterion, as will be explained in the following sections. The available power yield from a given heat sources is better described by the overall net efficiency given in Eq. (6).

3.2. Boiler efficiency

The boiler efficiency (calculated with Eq. (4)) of the two processes reacts in a fundamentally different way to a variation of the vapour pressure (Fig. 7). In the case of the improved ORC process, the boiler efficiency is significantly higher than that of the state-of-the-art process over the entire range of the vapour pressure. While boiler efficiency decreases significantly with increasing vapour pressure in the state-of-the-art process, it remains almost constant in the improved ORC process.

The decrease of the boiler efficiency with increasing vapour pressor at the turbine inlet at the state-of-the-art ORC process is based on two effects. First, a higher vapour pressure leads to a higher outlet temperature because the pinch point in the vapour generator is located at the end of the preheater and at the beginning of the evaporator. As a second effect, a higher vapour pressure leads to a higher superheating of the process fluid at the turbine exhaust, which means that the recuperator transfers a higher load of thermal power which increases the temperature of the process medium at the boiler feed. With the state-of-the-art ORC process, the maximum boiler efficiency of 68.21% is thus reached at a vapour pressure of 12 bar. With increasing vapour pressure, this drops by 26.3%$_{rel}$ to 53.99% at a pressure of 29 bar.

With the improved process the boiler efficiency curve is based on the following system behaviour. The boiler efficiency of the improved process is inherently higher because the degree of superheating of the process fluid is lower due to desuperheating by fluid injection and simultaneously the mass flow rate of the process fluid in the preheater is increased. The pressure dependency of the boiler efficiency is low, as the degree of superheating is lower compared to the state-of the-art process, since the desuperheating is carried out on the medium pressure stage. The resulting maximum boiler efficiency for the improved ORC process is 75.25% at a vapour pressure of 13 bar. As the vapour pressure increases, the boiler efficiency decreases slightly, by 2.4%$_{rel}$ to 73.51% at a pressure of 32 bar. The comparison of the maximum boiler efficiencies of the two processes leads to a relative difference of 10.3%$_{rel}$ in favour of the improved ORC process.

In addition to its contribution to the overall net efficiency, the boiler efficiency has another significance, which is illustrated in Fig. 8 for the constant boundary conditions shown in Table 1. With constant inlet conditions of the waste heat source (top right), the heat source can be utilised much better in the improved ORC process, which is noticeable not only in the increased transferred heat but also in a significantly lower temperature of the thermo oil flow at the vapour generator outlet. As a result, the waste heat source at the outlet of the thermo oil boiler also has a significantly lower temperature (see Fig. 9). This aspect has a direct influence on the dimensioning of downstream aggregates such as fans or filter systems due to a lower volume flow of the cooled down exhaust air after the thermo oil boiler. In addition to a cost saving due to

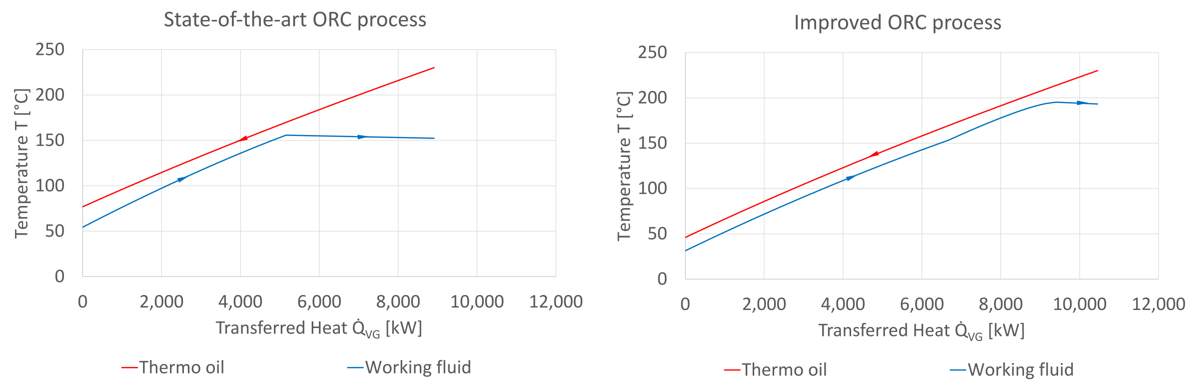

Fig. 8. Heat exchanger diagram of the vapour generator under optimum conditions of the state-of-the-art ORC process (left, vapour pressure $p_5 = 16.5$ bar) and the improved ORC process (right, vapour pressure $p_5 = 32$ bar).

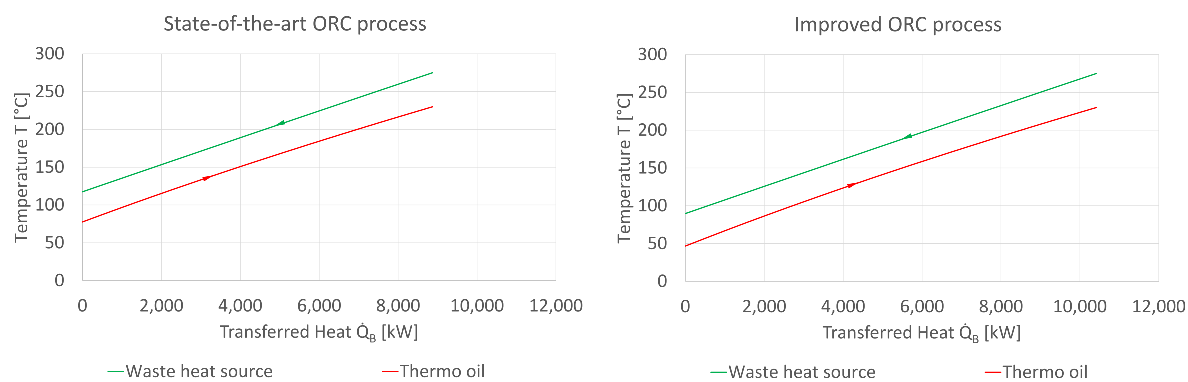

Fig. 9. Heat exchanger diagram of the thermooil boiler under optimum conditions of the state-of-the-art ORC process (left, vapour pressure $p_5 = 16.5$ bar) and the improved ORC process (right, vapour pressure $p_5 = 32$ bar).

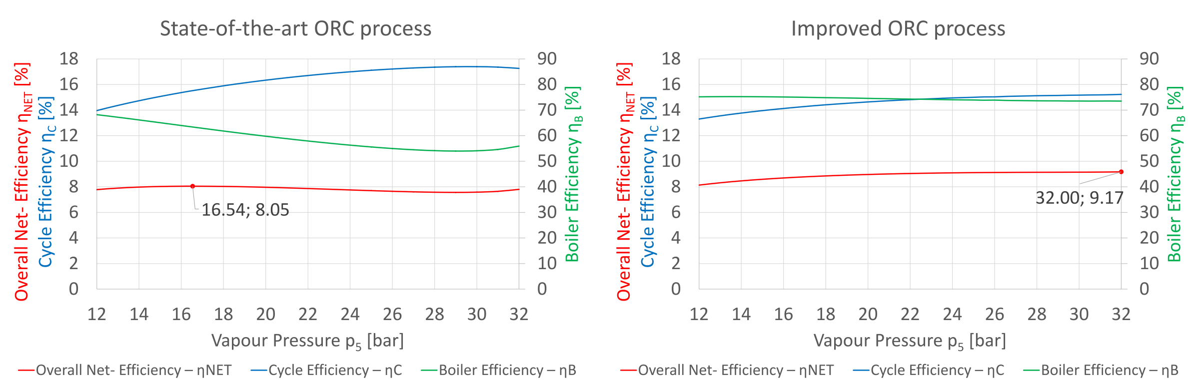

Fig. 10. Parameter study of the state-of-the-art ORC process (left) and the improved ORC process (right): Boiler efficiency, cycle efficiency and overall net efficiency as a function of vapour pressure at the high-pressure stage of the turbine. The pair of values shown in both graphs denotes the optimisation result for the overall net efficiency.

the reduced size of these units, there is also an additional energy saving due to the reduction of the volume flow of the draught fan.

3.3. Overall net efficiency

The overall net efficiency (as defined in Eq. (6)) is based on the available energy of the heat source. The simulation results show that cycle efficiency increases with increasing vapour pressure entering the high-pressure stage of the turbine (Fig. 10), which is to be expected thermodynamically. As the vapour pressure increases, the boiler efficiency decreases due to an increase in the output temperature of the waste heat source from the boiler. This effect is much more evident in the state-of-the-art ORC process than in the improved ORC process. The final result shows that with the state-of-the-art ORC process the maximum overall net efficiency is reached at a vapour pressure entering the high-pressure stage of the turbine of $p_5 = 16.5$ bar; the achieved overall net efficiency is $\eta_{NET} = 8.05\%$. With the improved ORC process the maximum overall net efficiency exceeds the respective values of the state-of-the art ORC at any pressure: at a vapour pressure of $p_5 = 20$ bar the relative increase of the overall net efficiency of the 11.4% is reached (Fig. 11). At the thermodynamically optimal vapour pressure of $p_5 = 32$ bar the improved ORC process reaches an overall net efficiency of $\eta_{NET} = 9.17\%$, which means an increase of the overall net efficiency of 14% relative to the state-of-the-art ORC process. This increase in the overall

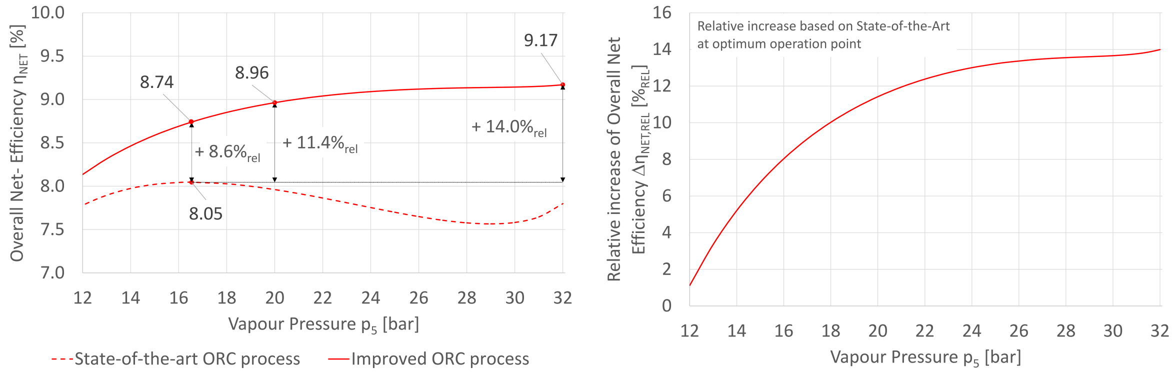

Fig. 11. Comparison of the overall net efficiency of the state-of-the-art ORC process and the improved ORC process at varying vapour pressure entering the high-pressure stage of the turbine (left), and increase of the net overall efficiency of the improved process relative to the state-of-the-art ORC process at optimum operation point (right).

Table 2
Simulation results at optimum operation point.

	State-of-the-art ORC process	Improved ORC process	Unit
Energy balance			
Waste heat input – temperature $T_{HS,IN}$	275	275	°C
Waste heat output – temperature $T_{HS,OUT}$	117	93	°C
Turbine high pressure stage – vapour pressure p_5	16.5	32.0	bar
Turbine medium pressure stage – vapour pressure p_7	–	9.0	bar
Turbine medium pressure stage – injected flow[a]	–	26.3	%
Thermo oil boiler – transferred heat $\dot{Q}_B$	8,875	10,259	kW
Vapour generator – transferred heat $\dot{Q}_{VG}$[b]	8,911	10,294	kW
Recuperator – transferred heat $\dot{Q}_R$	1,030	–	kW
Condenser – transferred heat $\dot{Q}_{CO}$	7,528	8,724	kW
Generator – electrical power $P_{EL,G}$	1,353	1,586	kW
Auxiliary units (Pumps + fans) – electr. power $P_{EL,A}$	227	304	kW
Electrical net power output $P_{EL,NET}$	1,126	1,282	kW
Efficiency			
Boiler efficiency – η_B	63.4	73.3	%
Cycle efficiency – η_C	15.5	15.3	%
Overall net efficiency – η_{NET}	8.05	9.17	%
Relative increase of Overall net efficiency – $\Delta\eta_{NET,REL}$	0	14	$\%_{REL}$

[a] Injected flow at the turbine medium pressure stage as a percentage of the live vapour mass flow at the high pressure stage of the turbine.
[b] The transferred heat of the vapour generator is higher than the transferred heat of the thermo oil boiler, as energy is supplied to the thermo oil circuit by the pump.

net efficiency of the process is mainly determined by the ability of the improved ORC process to lower the return temperature of the heat source.

The detailed simulation results of both variants are shown in Table 2. The results apply to the respective optimal vapour pressures for each process. In a realistic plant design, the vapour pressure is commonly chosen to be lower than the thermodynamically optimal pressure. Generally, the idea of the improved cycle favours the application of a higher pressure level on the working fluid side.

4. Conclusions

This study compares an improved ORC process with a state-of-the-art ORC process. The improved process calls for adaptations in the process design. A fluid flow is injected after the high-pressure stage of the turbine via a branch-off from the preheater of the vapour generator. This increases the mass flow through the preheater as well as the mass flow of the medium-pressure stage of the turbine. The recuperator, which is frequently used for dry class working fluids, can be omitted and is replaced by a spray condenser after the intermediate pressure stage of the turbine. Consequently, the condensation pressure decreases due to the elimination of the pressure drop of the recuperator and a higher enthalpy drop at the expansion turbine can be achieved. Although the cycle efficiency of the improved ORC process decreases slightly, the boiler efficiency increases significantly, and the heat source can be better utilised. Taken together, these effects lead to an increase in the overall net efficiency of up to 14% relative to the state-of-the-art ORC design, as determined at the optimal operating points of the respective process.

Declaration of competing interest

The authors declare that they have no known competing financial interests or personal relationships that could have appeared to influence the work reported in this paper.

Acknowledgement

The study was carried out as part of the Josef Ressel Centre for Linked System Assessment to Support Sustainable Energy Supplies (LiSA). Financial support by the Austrian Federal Ministry for Digital and Economic Affairs, by the National Foundation for Research, Technology and Development, by the Christian Doppler Research Association, and by the project partners Burgenland Energie AG and Wien Energie GmbH is gratefully acknowledged.

References

[1] Firth A, Zhang B, Yang A. Quantification of global waste heat and its environmental effects. Appl Energy 2019;235:1314–34. https://doi.org/10.1016/j.apenergy.2018.10.102.

[2] Brueckner S, Miró L, Cabeza LF, Pehnt M, Laevemann E. Methods to estimate the industrial waste heat potential of regions - a categorization and literature review. Renew Sustain Energy Rev 2014;38:164–71. https://doi.org/10.1016/j.rser.2014.04.078.

[3] Miró L, Brückner S, Cabeza LF. Mapping and discussing Industrial Waste Heat (IWH) potentials for different countries. Renew Sustain Energy Rev 2015;51:847–55. https://doi.org/10.1016/j.rser.2015.06.035.

[4] Su Z, Zhang M, Xu P, Zhao Z, Wang Z, Huang H, et al. Opportunities and strategies for multigrade waste heat utilization in various industries: a recent review. Energy Convers Manag 2021;229. https://doi.org/10.1016/j.enconman.2020.113769.

[5] Campana F, Bianchi M, Branchini L, De Pascale A, Peretto A, Baresi M, et al. ORC waste heat recovery in European energy intensive industries: energy and GHG savings. Energy Convers Manag 2013;76:244–52. https://doi.org/10.1016/j.enconman.2013.07.041.

[6] Tartière T, Astolfi M. A world overview of the organic rankine cycle market. Energy Proc 2017;129:2–9. https://doi.org/10.1016/j.egypro.2017.09.159.
[7] Wieland C, Dawo F, Schifflechner S, Astolfi M. Market report on organic rankine cycle power systems: recent development and outlook. In: Orc 2021 - 6th int. Semin. ORC power syst., munich; 2021. https://doi.org/10.14459/2021mp1636584.
[8] Lecompte S, Huisseune H, van den Broek M, Vanslambrouck B, De Paepe M. Review of organic Rankine cycle (ORC) architectures for waste heat recovery. Renew Sustain Energy Rev 2015;47:448–61. https://doi.org/10.1016/j.rser.2015.03.089.
[9] Loni R, Najafi G, Bellos E, Rajaee F, Said Z, Mazlan M. A review of industrial waste heat recovery system for power generation with Organic Rankine Cycle: recent challenges and future outlook. J Clean Prod 2021;287. https://doi.org/10.1016/j.jclepro.2020.125070.
[10] Feng Y, Hung TC, Greg K, Zhang Y, Li B, Yang J. Thermoeconomic comparison between pure and mixture working fluids of organic Rankine cycles (ORCs) for low temperature waste heat recovery. Energy Convers Manag 2015;106:859–72. https://doi.org/10.1016/j.enconman.2015.09.042.
[11] Exergy International Srl. Technology - organic rankine cycle 2021. https://www.exergy-orc.com/orc. [Accessed 20 January 2021]. accessed.
[12] Center for promotion of sustainable energy Velika Ciglena geothermal power plant starts operation 2018. accessed https://balkangreenenergynews.com/velika-ciglena-geothermal-power-plant-starts-operation/. [Accessed 20 January 2021].
[13] Li YM, Hung TC, Wu CJ, Su TY, Xi H, Wang CC. Experimental investigation of 3-kW organic Rankine cycle (ORC) system subject to heat source conditions: a new appraisal for assessment. Energy 2020;217:119342. https://doi.org/10.1016/j.energy.2020.119342.
[14] Vaccaro M, Franco A. Recent trends in research and application of ORC plants for geothermal energy use. Eur. Geotherm. Congr. 2016 Strasbourg: 2016.
[15] White MT, Sayma AI. Fluid selection for small-scale rankine cycle plants: can you draw some lines in the sand?. In: Int. Rank. 2020 conf. -Heating, cool. Power gener., vol. 2020- july, Glasgow; 2020. p. 305–10. https://doi.org/10.18462/iir.rankine.2020.1161.
[16] Darvish K, Ehyaei MA, Atabi F, Rosen MA. Selection of optimum working fluid for organic rankine cycles by exergy and exergy-economic analyses. Sustain Times 2015;7:15362–83. https://doi.org/10.3390/su71115362.
[17] Zhou Y, Wu Y, Li F, Yu L. Performance analysis of zeotropic mixtures for the dual-loop system combined with internal combustion engine. Energy Convers Manag 2016;118:406–14. https://doi.org/10.1016/j.enconman.2016.04.006.
[18] Zhi LH, Hu P, Chen LX, Zhao G. Performance analysis and optimization of engine waste heat recovery with an improved transcritical-subcritical parallel organic Rankine cycle based on zeotropic mixtures. Appl Therm Eng 2020;181. https://doi.org/10.1016/j.applthermaleng.2020.115991.
[19] Wang S, Yuan Z. A hot water split-flow dual-pressure strategy to improve system performance for organic Rankine cycle. Energies 2020;13. https://doi.org/10.3390/en13133345.
[20] Wang M, Zhang J, Zhao S, Liu Q, Zhao Y, Wu H. Performance investigation of transcritical and dual-pressure Organic Rankine Cycles from the aspect of thermal match. Energy Convers Manag 2019;197. https://doi.org/10.1016/j.enconman.2019.111850.
[21] Boodaghi H, Etghani MM, Sedighi K. Performance analysis of a dual-loop bottoming organic Rankine cycle (ORC) for waste heat recovery of a heavy-duty diesel engine, Part I: thermodynamic analysis. Energy Convers Manag 2021:113830. https://doi.org/10.1016/j.enconman.2021.113830.
[22] Emadi MA, Chitgar N, Oyewunmi OA, Markides CN. Working-fluid selection and thermoeconomic optimisation of a combined cycle cogeneration dual-loop organic Rankine cycle (ORC) system for solid oxide fuel cell (SOFC) waste-heat recovery. Appl Energy 2020;261. https://doi.org/10.1016/j.apenergy.2019.114384.
[23] Valencia G, Fontalvo A, Duarte Forero J. Optimization of waste heat recovery in internal combustion engine using a dual-loop organic Rankine cycle: thermo-economic and environmental footprint analysis. Appl Therm Eng 2021:182. https://doi.org/10.1016/j.applthermaleng.2020.116109.
[24] Song J, Li X, Wang K, Markides CN. Parametric optimisation of a combined supercritical CO2 (S-CO2) cycle and organic Rankine cycle (ORC) system for internal combustion engine (ICE) waste-heat recovery. Energy Convers Manag 2020;218. https://doi.org/10.1016/j.enconman.2020.112999.
[25] Mohammed AG, Mosleh M, El-Maghlany WM, Ammar NR. Performance analysis of supercritical ORC utilizing marine diesel engine waste heat recovery. Alex Eng J 2020;59:893–904. https://doi.org/10.1016/j.aej.2020.03.021.
[26] Hassani Mokarram N, Mosaffa AH. Investigation of the thermoeconomic improvement of integrating enhanced geothermal single flash with transcritical organic Rankine cycle. Energy Convers Manag 2020;213. https://doi.org/10.1016/j.enconman.2020.112831.
[27] Witanowski, Klonowicz P, Lampart P, Suchocki T, Jędrzejewski Zaniewski D, et al. Optimization of an axial turbine for a small scale ORC waste heat recovery system. Energy 2020;205. https://doi.org/10.1016/j.energy.2020.118059.
[28] Chatzopoulou MA, Lecompte S, Paepe M De, Markides CN. Off-design optimisation of organic Rankine cycle (ORC) engines with different heat exchangers and volumetric expanders in waste heat recovery applications. Appl Energy 2019;253. https://doi.org/10.1016/j.apenergy.2019.113442.
[29] Xu R-J, He Y-L. A vapor injector-based novel regenerative organic Rankine cycle. Appl Therm Eng 2011;31:1238–43. https://doi.org/10.1016/j.applthermaleng.2010.12.026.
[30] Hernandez A, Desideri A, Ionescu C, Quoilin S, Lemort V, De Keyser R. Increasing the efficiency of organic rankine cycle technology by means of multivariable predictive control. IFAC Proc 2014;19:2195–200. https://doi.org/10.3182/20140824-6-za-1003.01796.
[31] Baccioli A, Antonelli M. Control variables and strategies for the optimization of a WHR ORC system. Energy Proc 2017;129:583–90. https://doi.org/10.1016/j.egypro.2017.09.212.
[32] Zhang J, Li K, Xu J. Recent developments of control strategies for organic Rankine cycle (ORC) systems. Trans Inst Meas Control 2019;41:1528–39. https://doi.org/10.1177/0142331217753061.
[33] Imran M, Pili R, Usman M, Haglind F. Dynamic modeling and control strategies of organic Rankine cycle systems: methods and challenges. Appl Energy 2020:276. https://doi.org/10.1016/j.apenergy.2020.115537.
[34] Heberle F. Untersuchungen zum Einsatz von zeotropen Fluidgemischen im Organic Rankine Cycle für die geothermische Stromerzeugung. Berlin: Logos Verlag; 2013.
[35] Su W, Hwang Y, Deng S, Zhao L, Zhao D. Thermodynamic performance comparison of Organic Rankine Cycle between zeotropic mixtures and pure fluids under open heat source. Energy Convers Manag 2018;165:720–37. https://doi.org/10.1016/j.enconman.2018.03.071.
[36] Dong B, Xu G, Luo X, Zhuang L, Quan Y. Potential of low temperature organic rankine cycle with zeotropic mixtures as working fluid. Energy Proc 2017;105:1489–94. https://doi.org/10.1016/j.egypro.2017.03.444.
[37] Dong B, Xu G, Li T, Quan Y, Wen J. Thermodynamic and economic analysis of zeotropic mixtures as working fluids in low temperature organic Rankine cycles. Appl Therm Eng 2018;132:545–53. https://doi.org/10.1016/j.applthermaleng.2017.12.083.
[38] Modi A, Haglind F. A review of recent research on the use of zeotropic mixtures in power generation systems. Energy Convers Manag 2017;138:603–26. https://doi.org/10.1016/j.enconman.2017.02.032.
[39] Collings P, Yu Z, Wang E. A dynamic organic Rankine cycle using a zeotropic mixture as the working fluid with composition tuning to match changing ambient conditions. Appl Energy 2016;171:581–91. https://doi.org/10.1016/j.apenergy.2016.03.014.
[40] Beckmann G. Verfahren und Einrichtung zur Erzeugung von Kälte und/oder Nutzwärme sowie mechanischer bzw. elektrischer Energie mittels eines Absorptionskreislaufes. Austrian Patent 2012;AT511823B1.
[41] Chen T, Zhuge W, Zhang Y, Zhang L. A novel cascade organic Rankine cycle (ORC) system for waste heat recovery of truck diesel engines. Energy Convers Manag 2017;138:210–23. https://doi.org/10.1016/j.enconman.2017.01.056.
[42] Tchanche BF, Lambrinos G, Frangoudakis A, Papadakis G. Low-grade heat conversion into power using organic Rankine cycles – a review of various applications. Renew Sustain Energy Rev 2011;15:3963–79. https://doi.org/10.1016/j.rser.2011.07.024.
[43] Peñate B, García-Rodríguez L. Seawater reverse osmosis desalination driven by a solar Organic Rankine Cycle: design and technology assessment for medium capacity range. Desalination 2012;284:86–91. https://doi.org/10.1016/j.desal.2011.08.040.
[44] Larsen U, Pierobon L, Haglind F, Gabrielii C. Design and optimisation of organic Rankine cycles for waste heat recovery in marine applications using the principles of natural selection. Energy 2013;55:803–12. https://doi.org/10.1016/j.energy.2013.03.021.
[45] Moloney F, Almatrafi E, Goswami DY. Working fluid parametric analysis for recuperative supercritical organic Rankine cycles for medium geothermal reservoir temperatures. Renew Energy 2020;147:2874–81. https://doi.org/10.1016/j.renene.2018.09.003.
[46] Beckmann G, Krail J. Verfahren zur Steigerung der Energieeffizienz in Clausius-Rankine-Kreisprozessen. AT521050B1. 2019.
[47] Krail J, Beckmann G. Verfahren und Vorrichtung zur Wandlung von thermischer in mechanische bzw. elektrische Energie. WO2019/227117A1. 2019.
[48] Baehr HD, Kabelac S. Thermodynamik. Berlin, Heidelberg: Springer Berlin Heidelberg; 2016. https://doi.org/10.1007/978-3-662-49568-1.
[49] SimTech GmbH. IPSEpro - software system for calculating heat balances and simulating processes 2021. http://www.simtechnology.com/CMS/index.php/ipsepro. [Accessed 23 June 2021]. accessed.
[50] SimTech GmbH. IPSEpro LTP_Lib - low temperature process library. 2016.
[51] NIST - National Institute of Standards and Technology. Refprop - NIST reference fluid thermodynamic and transport properties. 2013.
[52] SimTech GmbH. IpsePro PSE - process simulation environment. 2017.
[53] SimTech GmbH. IpsePro process simulation environment (manual version 6.0.001). Graz; 2014.
[54] SimTech GmbH. IPSEpro PSOptimize - parameter optimization. 2014.
[55] SimTech GmbH. IPSEPro PSXLink - integration with microsoft Excel. 2017.
[56] Heidelberger Cement AG. Niedertemperaturverstromung mittels einer ORC-Anlage im Werk Lengfurt der Heidelberger Zement AG. Augsburg; 2001.
[57] Umweltbundesamt. Merkblatt über die Besten Verfügbaren Techniken in der Zement-, Kalk- und Magnesiumoxidindustrie. Dessau; 2010.
[58] Vdz - Verein Deutscher Zementwerke eV. Zement taschenbuch. Düssendorf. Verlag Bau+Technik GmbH; 2002.
[59] Strauss K. Kraftwerkstechnik. Berlin, Heidelberg: Springer Berlin Heidelberg; 2016. https://doi.org/10.1007/978-3-662-53030-6.
[60] von Böckh P, Stripf M. Thermische energiesysteme. Berlin, Heidelberg: Springer Berlin Heidelberg; 2018. https://doi.org/10.1007/978-3-662-55335-0.